



**HAL**  
open science

# Mineral waste valorization in road subgrade construction: Algerian case study based on technical and environmental features

Selma Bellara, Walid Maherzi, S. Mezazigh, Ahmed Senouci

## ► To cite this version:

Selma Bellara, Walid Maherzi, S. Mezazigh, Ahmed Senouci. Mineral waste valorization in road subgrade construction: Algerian case study based on technical and environmental features. *Case Studies in Construction Materials*, 2024, 20, pp.e02764. 10.1016/j.cscm.2023.e02764 . hal-04495189

**HAL Id: hal-04495189**

**<https://hal.science/hal-04495189>**

Submitted on 13 Mar 2024

**HAL** is a multi-disciplinary open access archive for the deposit and dissemination of scientific research documents, whether they are published or not. The documents may come from teaching and research institutions in France or abroad, or from public or private research centers.

L'archive ouverte pluridisciplinaire **HAL**, est destinée au dépôt et à la diffusion de documents scientifiques de niveau recherche, publiés ou non, émanant des établissements d'enseignement et de recherche français ou étrangers, des laboratoires publics ou privés.



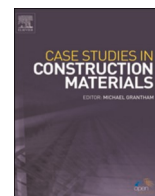
Distributed under a Creative Commons Attribution 4.0 International License



ELSEVIER

Contents lists available at ScienceDirect

## Case Studies in Construction Materials

journal homepage: [www.elsevier.com/locate/cscm](http://www.elsevier.com/locate/cscm)

## Case study

# Mineral waste valorization in road subgrade construction: Algerian case study based on technical and environmental features

Selma Bellara<sup>a,b,c</sup>, Walid Maherzi<sup>b,\*</sup>, Salim Mezazigh<sup>c</sup>, Ahmed Senouci<sup>d</sup>

<sup>a</sup> Materials, Geotechnics, Housing and Urban Planning Laboratory (LMGHU), Faculty of technology, University of 20 aout 1955-Skikda, 26 Route d'El-Hadaiek, Skikda 21000, Algeria

<sup>b</sup> Univ. Lille, IMT Nord Europe, Univ. Artois, JUNIA, ULR 4515 - LGCgE, Laboratory of Civil Engineering and Geo-Environment, F-59000 Lille, France

<sup>c</sup> Continental and Coastal Morphodynamics Laboratory (M2C), UMR 6143 CNRS, University Caen Normandie, 24 Rue des Tilleuls, F-14000 Caen, France

<sup>d</sup> Department of Construction Management College of Technology Building, 4730 Calhoun Road #300, Houston, TX 77204-4020, USA

## ARTICLE INFO

## Keywords:

Sediment  
Marble waste  
Granular corrector  
Road construction  
Circular economy  
Greenhouse emission

## ABSTRACT

This study has focused on the dam sediments and marble waste reuse as subgrade materials for road construction, with the overarching goals of reducing greenhouse gas emissions and conserving natural resources. Different mixtures were prepared based on sediments and marble waste, and treated with hydraulic binders. The first mixture consisted solely of raw sediment, while the second mixture combined 50 % dredged sediments with 50 % marble waste. Additionally, this mixture was treated with 1 % aerial hydrated lime and hydraulic road binder to enhance its properties. The experimental study focused on assessing both the short-term and long-term mechanical properties of the prepared mixtures. Results highlighted that the mixtures containing dam sediments and marble waste were highly suitable for road subgrade construction. These mixtures satisfied the criteria for trafficability (UCS), wetting resistance (UCSI), freezing resistance (ITS), and overall mechanical strength. Furthermore, a comprehensive analysis of the mixtures' microstructure and their environmental impact was conducted. A significant relationship was observed between CaO/SiO<sub>2</sub> ratio and the mechanical properties of the treated mix. The research contributes to the growing body of knowledge regarding sustainable construction practices by highlighting the viability of utilizing dredged sediments and marble waste as valuable resources in road subgrade construction. The study showed that recovering 20 % of sediment and marble waste to replace natural materials would reduce energy consumption and greenhouse gas emissions by at least 40 % and 28 % respectively.

## 1. Introduction

The construction industry is a significant consumer of raw materials and energy worldwide, accounting for half of the world's energy consumption [1,2]. In Algeria, it consumes a third of the country's total energy [3]. Furthermore, this industry is a major contributor to carbon emissions [2,4], responsible for 31 % of Algeria's greenhouse gas emissions [3]. Additionally, the construction sector heavily relies on natural aggregates, with a global consumption of 48.3 billion metric tons in 2015 [5]. The depletion and

\* Corresponding author.

E-mail address: [walid.maherzi@imt-nord-europe.fr](mailto:walid.maherzi@imt-nord-europe.fr) (W. Maherzi).

<https://doi.org/10.1016/j.cscm.2023.e02764>

Received 7 September 2023; Received in revised form 26 November 2023; Accepted 3 December 2023

Available online 5 December 2023

2214-5095/© 2023 The Authors. Published by Elsevier Ltd. This is an open access article under the CC BY license (<http://creativecommons.org/licenses/by/4.0/>).

overconsumption of these natural resources raises serious concerns for the industry's future. Thus, the development of cost-effective alternatives to natural raw materials becomes critical for the success of construction projects.

Currently, North African dams are grappling with high sedimentation levels, with over 20 million m<sup>3</sup> of sediments being deposited annually in Algerian dams [6]. On a global scale, hundreds of million tons of sediments are dredged each year [7]. Researchers have explored various sediment valorization approaches for civil engineering applications, including road pavements [8–12], bricks [13, 14], sand substitutions [15,16], Supplementary Cementitious Materials (SCMs) [17,18], Self-Consolidating Concrete (SCC) [19,20], geopolymer binders [21,22], asphalt applications [23], and even agricultural uses [24]. These valorized sediments have found application in several large-scale construction projects worldwide, such as the French Waterways, Rotterdam Port, London National Theatre, Great Belt Link between Denmark and Sweden, and Dubai Palm Island [25]. To effectively utilize these sediments in specific civil engineering applications, it is crucial to understand their physical, geotechnical, and mechanical properties, as well as conduct environmental assessments to ensure their safety and compatibility with the environment. Several sediment management laws and regulations have already been established to address their environmental impact. By promoting the use of dredged sediments and waste as alternative solutions, the sustainable management of construction raw materials can be achieved, offering economic and ecological advantages while preserving non-renewable natural resources and reducing carbon footprints.

Notably, Algeria stands out as a leading producer and manufacturer of high-quality marble in Africa [26]. Marble, a metamorphic rock formed from limestone under heat and metamorphic pressure [24], consists mainly of mineral calcite (CaCO<sub>3</sub>) and other secondary minerals, including clay minerals, micas, quartz, pyrite, iron oxides, and graphite [27]. Throughout history, marble has been used for building sculptures and statues by ancient Greeks and Romans. However, the current excessive production of marble generates substantial amounts of powder and sand waste during the production process.

Algeria has historically exhibited a significant production capacity for marble and granite, reaching up to 30,000 tons in the past. However, the current production has declined to 14,000 tons [28]. About 70 % of this mineral is wasted in the processes of mining, processing, and polishing [29]. The ongoing excessive production of marble has resulted in a significant accumulation of powder and sand waste, posing environmental challenges during manufacturing, extraction, and processing operations [27]. In response to this issue, researchers have recognized the potential of utilizing marble waste as an alternative construction material, presenting economic and environmental advantages [30–34]. This article investigates the viability of incorporating marble waste and dredged sediments in the construction of road subgrades. To achieve this, two key approaches were employed: (1) introducing marble waste with a maximum particle size of 2 mm into the sediment granular structure, optimizing mix packing densities using the Talbot-Fuller-Thompson method; (2) conducting sediment mix designs, comparing the presence and absence of marble waste as granular correction, applying the Talbot-Fuller-Thomson optimization method. The determination of lime and hydraulic road binder percentages followed the Lime Fixing Point (LFP) test recommendations and the subgrade and road construction French guide (GTS) standards. Extensive testing was carried out to assess the road subgrade construction suitability of the prepared mixes, with additional leaching tests to evaluate their environmental safety.

## 2. Research significance

Over the last few years, the significant number papers on the subject of using wastes in road construction were published. The aim of previous study was to replace only a fraction of the natural materials [8;45;47;51;53]. The main aim of our study was to investigate the feasibility of use mixes based on dam sediments and marble waste, and treated with hydraulic road binders comprised on calcined sediment dam and blast furnace slag, as subgrade materials for road construction. Experimental analyses such as mechanical properties (UCS and ITS), resistance to water immersion, mercury intrusion porosimeter (MIP), and microstructure analyses (SEM observation) were used to investigate the impact of marble waste and hydraulic binders' treatment on road materials. The obtained results in this study that enhanced understanding of the use only mineral wastes in the road materials mixtures. Indeed, the impact of the CaO/SiO<sub>2</sub> ratio of the hydraulic binders, and the packing density of the mixtures on the mechanical performances was defined. Furthermore, the impact of the use of mineral waste on greenhouse gas emissions and fossil energy consumption was highlighted.

**Table 1**

Binder physical, chemical, and mechanical properties.

Physical requirements NF EN 196-6. 3												
Residue by mass at 90 μm (%)			Initial setting time (min)			Expansion (mm)						
HRB-1	HRB-2	Limit	HRB-1	HRB-2	Limit	HRB-1	HRB-2	Limit				
0.28	0.18	≤ 15	230	250	≥ 150	1.28	0.74	≤ 30				
Chemical requirements NF EN 196-2												
SO <sub>3</sub> content (%)			Compressive strength at 56 days (MPa) NF EN 13282-2									
HRB-1	HRB-2	Limit	HRB-1		HRB-2							
1.28	0.74	4.00	50.06		54.18							
			Strength class N4									
HRB-1	HRB-2	FeO <sub>3</sub>	CaO	MgO	SO <sub>3</sub>	K <sub>2</sub> O	Na <sub>2</sub> O	TiO <sub>2</sub>	MnO	BaO	SrO	OF <sub>2</sub>
24.26	6.86	3.40	57.89	1.38	3.76	1.28	0.32	0.41	0.16	0.17	0.03	0.09
HRB-2	HRB-2	FeO <sub>3</sub>	CaO	MgO	SO <sub>3</sub>	K <sub>2</sub> O	Na <sub>2</sub> O	TiO <sub>2</sub>	MnO	BaO	SrO	OF <sub>2</sub>
30.38	8.44	2.98	49.39	2.34	2.82	1.38	0.31	0.42	0.55	0.58	0.09	0.31

### 3. Materials and methods

#### 3.1. Materials

##### 3.1.1. Hydraulic road binders (HRB)

The hydraulic road binders were composed of three main constituents: cement CEM I 42.5 N, blast furnace slag, and calcined sediments, combined in varying proportions. The initial binder, denoted as HRB-1, comprised 80 % cement, 10 % blast furnace slag, and 10 % calcined sediments. In contrast, the second binder, labeled HRB-2, contained 50 % cement, 35 % blast furnace slag, and 15 % calcined sediments. Detailed information regarding the physical, chemical, and mechanical properties of these binders, along with the standard requirements (EN 13282-2) for normally hardened hydraulic road binders, can be found in Table 1 [9]. Additionally, Fig. 1 presents the binder grain size distributions.

##### 3.1.2. Hydrated lime (HL)

For the mix treatment, a hydrated lime powder (CL 90-S) was employed, possessing an absolute density of  $2.31 \text{ g/cm}^3$ . The lime powder adhered to strict standards, as outlined in EN 459-1 and NF P98-101, ensuring a minimum of 90 % free lime (CaO) content and a maximum of 5 % magnesium oxide (MgO) content. Fig. 1 illustrates the particle size distribution of the lime, revealing that the maximum particle size was less than  $80 \mu\text{m}$ .

##### 3.1.3. Raw sediments

The sediments were sourced from Zardezas dam in northeastern Algeria, a location facing a significant risk of short-term total siltation, evident by its current storage, which is now less than a quarter of its initial capacity [35]. Multiple samples were manually collected from depths ranging between 0 and 70 cm. These samples were then subjected to a series of preparation steps, including air-drying, oven drying at  $50^\circ\text{C}$  for 48 h, crushing, homogenization, and storage in sealed plastic bags.

To comprehensively assess the sediment properties, various physical, chemical, geotechnical, mechanical, and environmental analyses were conducted following French and European standards. A summary of the obtained results is presented in Table 2. Based on the SETRA-LCPC technical guide [36], the sediments were categorized as belonging to class A3 and sub-class F11, exhibiting an organic matter content ranging from 3 % to 10 %. Remarkably, Fergoug's and Bakhadda's dam sediments also fall into the same class [37,38], indicating similarities in their characteristics.

The X-ray diffraction (XRD) patterns further unveiled the composition of the dam sediments, revealing three primary crystalline phases: clay minerals (Kaolinite, Illite, Chlorite, and Albite), silicates (Quartz), and carbonate (dolomite and calcite) (Fig. 2). Remini [39] has also reported similar crystalline phases for these sediments in his research, reinforcing the consistency of the findings.

The scanning electron microscope (SEM) images were captured using a Hitachi S-4300SE/N Electron Microscope, which was equipped with a Thermo-Scientific Ultradry EDX detector. Fig. 3(a) exhibits the morphology of the fine porous particles and the layered structure of the clays found in the raw sediments. In Fig. 3(b), framboidal pyrite is observed in the mineralogical composition of the raw sediments. These noteworthy findings align with previous studies conducted on marine and river sediments [8,40–42], wherein hydraulic treatment in the presence of calcium aluminate and calcium silicate hydrates was applied. Notably, the presence of pyrite can induce the formation of expansive products, such as ettringite and thaumasite. The layered clay mineral structure is displayed in Fig. 3(c).

Table 3 summarizes the raw sediment chemical composition, which consists of Silicate (Si), Aluminum (Al), Calcium (Ca), and Iron (Fe).

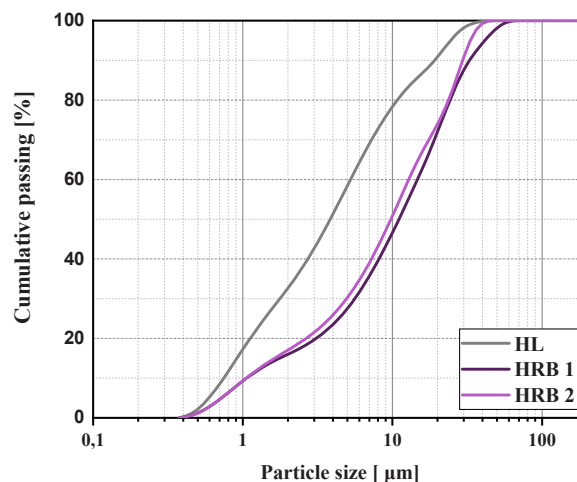


Fig. 1. Hydrated lime and hydraulic road binder particle size distribution.

**Table 2**  
Zardezas dam sediment characteristics.

Properties	Standards	Sediments
Initial water content (%)	NF P94-050	47–57
Laser granulometric analysis (Wet method):	ISO 13320-1	
Fine particles (% < 80 $\mu\text{m}$ )		90
Clayey fraction $D_{\text{max}} < 2 \mu\text{m}$ (%)		34.25
Silty fraction $2 \mu\text{m} < D_{\text{max}} < 63 \mu\text{m}$ (%)		54
Sandy fraction $63 \mu\text{m} < D < 2 \text{mm}$ (%)		11.75
Absolute density ( $\text{g}/\text{cm}^3$ )	NF EN 1097-7	2.63
Organic matter content at 450 °C	XP P 94-047	3.67
Loss on ignition at 550 °C	NF EN 15169	6.29
Blue methylene value ( $\text{g}/100 \text{g}$ )	NF P 94-068	4.41
Liquid limit (%)	NF P94-051	52.1
Plastic limit (%)	NF P94-051	22.2
Plasticity index (%)		29.9
$\text{CaCO}_3$ content	NF P 94-048	15.55
pH value	NF ISO 10390	8.4
Proctor test	NF P94-093	
Maximal dry density ( $\text{t}/\text{m}^3$ )		1.58
Optimum water content (%)		23
Immediate bearing index (%)	NF P94-078	7.11
Leaching test	EN 12457-2	Inert (French Directive of 14 December 2014)
Class	SETRA-LCPC	A <sub>3</sub> F <sub>11</sub>

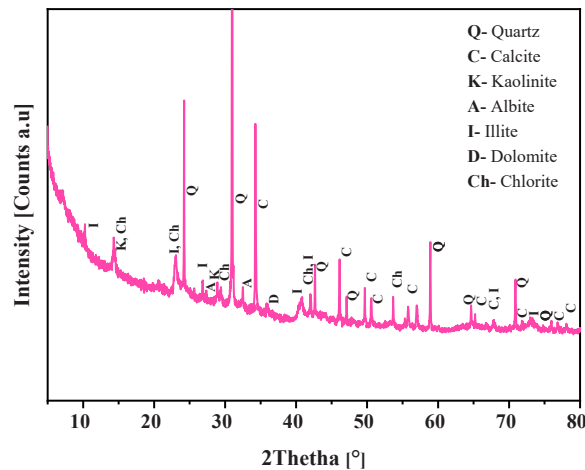


Fig. 2. Zardezas dam sediment XRD patterns.

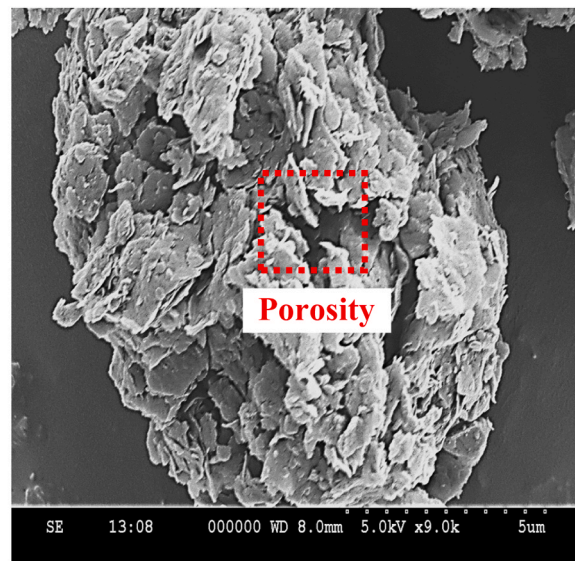
### 3.1.4. Marble waste

The granular corrector employed in this study was derived from the marble sandy waste extracted from Skikda's CHATT/Fil-Fila quarry in northeastern Algeria (<https://www.enamarbre.dz>). The particle sizes of this waste material ranged from 0 to 2 mm, surpassing the raw sediments in coarseness. Fig. 4 illustrates the morphology and particle size distribution of the marble waste, as obtained through SEM analysis in BSE and SE modes, utilizing an accelerating voltage of 15.0 and 5.0 KV, along with a working distance of 10.0 mm.

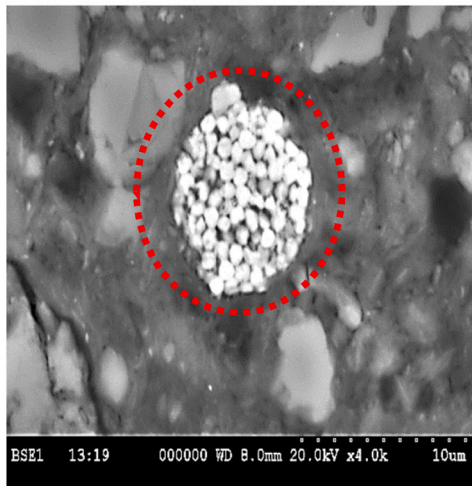
## 3.2. Methods

### 3.2.1. Dam sediment granular skeleton binder dosage optimization

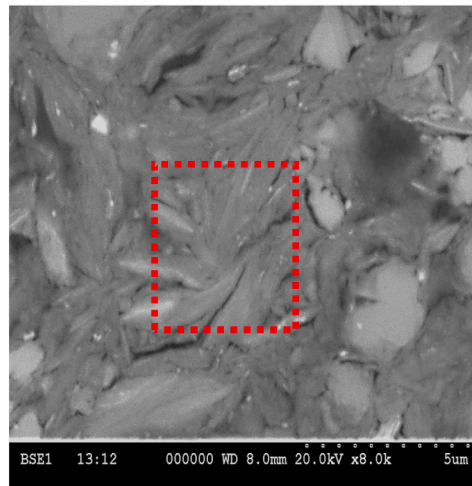
**3.2.1.1. Granular correction.** Even when compacted, dredged sediments lack sufficient strength and stiffness for road applications. Consequently, the addition of chemical admixtures is undertaken to enhance their properties [43]. With an IBI of  $7.11 < 10$ , required for use as a subgrade for A3 classes, the Zardezas sediments are not suitable for direct utilization and necessitate a combined treatment with lime and hydraulic binders. The prescribed treatment involves 1 % lime and 7 % hydraulic binders, adhering to the specifications of the French technical guide GTS.



(a)



(b)



(c)

Fig. 3. (a) Sediment grain SE mode morphology, (b) framboidal pyrite, (c) layered clay mineral structure.

**Table 3**

Zarzedas dam sediments X-ray fluorescence results.

Major oxide	SiO <sub>2</sub>	Al <sub>2</sub> O <sub>3</sub>	FeO <sub>3</sub>	CaO	MgO	SO <sub>3</sub>	K <sub>2</sub> O	Na <sub>2</sub> O	TiO <sub>2</sub>
Percentage (%)	48.27	17.73	6.26	9.35	2.11	Traces	2.25	0.36	0.81

Previous literature suggests that sediments treated solely with binders can achieve a porosity of approximately 50 %, resulting in diminished mechanical properties [44]. However, it has been demonstrated that incorporating a granular corrector alongside hydraulic binders enhances both the physical and mechanical characteristics of the sediments [45,46]. To achieve this improvement, a granular skeleton for the mixtures was developed using the semi-empirical Talbot-Fuller-Thompson (T-F-T) method. The objective was twofold: firstly, to reduce the porosity of Zarzedas dam sediments, and secondly, to optimize their packing density while attaining suitable mechanical properties for road subgrade application, thereby minimizing binder content [47]. The application of Fuller's reference curves typically ensures an optimum packing density gradation. By employing granulometric curves, bounded by two theoretical T-F-T curves obtained through Eq. (1), the most favorable grain arrangement with minimal porosity can be achieved.



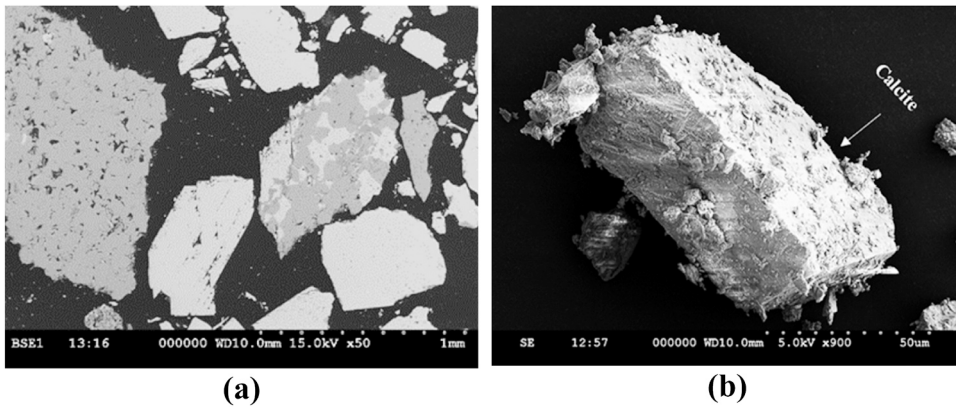


Fig. 4. Sandy marble waste SEM micrographs (a) BSE mode (b) SE mode.

$$P = \left[ \frac{d}{D} \right]^n \quad (1)$$

Where: P = passing in sieve d (%), d = sieving diameter (mm), D = maximal grain diameter (mm), and n = grading or adjustment coefficient with a value between 0.25 and 0.45.

**3.2.1.2. Lime fixation point (LFP).** The lime content required to achieve a pH of 12.4 was determined through the lime fixation point test, following the methods of Eades and Grim [48], and the French standard NF ISO 10390. It is important to highlight that a pH of 12.4 promotes both pozzolanic activity and hydrate precipitation [49]. For the assessment of the pH in the sediments and the 50 % SED and 50 % MW mix, a solid to water ratio of 1/5 was utilized. The pH of the mix was examined after incorporating various lime doses, as well as in the pre-humidified (D-1) state, with a 23 % water content (OWC).

The reaction of the mix lasted for one hour, during which water was added to achieve a solid to liquid ratio of 1/5, followed by one hour of agitation. To measure the pH, a calibrated meter was employed, and the assessments were conducted at a room temperature of 20 °C. The pH value recorded was stable within a variation of only 0.02 over one minute.

### 3.2.2. Mechanical properties

Table 4 summarizes all the mechanical tests carried out. Mixtures were pre-humidified, mixed with a mixer until homogenization and kept sealed in plastic bags for at least 24 h. The following day, mixture was placed in the mixer tank, mixed with lime for about 3 min then left to react for an hour. The road hydraulic binder was then incorporated, mixed for 5 min then poured into the Proctor mould and compacted in three layers with Normal Proctor energy (top of each layer was slightly scarified) following the French standards NF P94-093, to determine the Optimum Water Content and the maximum dry density. Immediate Bearing Index tests were conducted and NF P94-078, respectively, using an automatic loading machine with a capacity of 150 kN. The application of force on the penetration piston, characterized by a cross-sectional area of 1932 mm<sup>2</sup>, occurred at a penetration rate of approximately 1.27 mm min<sup>-1</sup>.

To evaluate the suitability of the mixes as alternative materials for road sublayer use, the French GTS guide [50] was employed. The assessment involved various tests, including treatment ability (NF P94-100), unconfined compressive strength (UCS) (NF EN 13286-41), wetting resistance (UCS<sub>w</sub>), freezing resistance (Rt) (NF EN 13286-42), as well as elastic modulus and tensile strength measurements. For each test, three cylindrical specimens were prepared from each mix. The mixes were pre-humidified and kept in sealed plastic bags. After 24 h, lime was added to the mixes, followed by 3 min of mixing. The mixes were then allowed to react for 1 h while conserved in sealed bags. Subsequently, a hydraulic road binder was added, and the mixes were mixed for another 5 min.

Cylindrical specimens with a diameter (D) of 50 mm and a depth (H) of 50 mm were prepared with OWC and a relative compaction degree of  $\rho = 0.96\text{x}\rho_d$ . These specimens were compacted according to the standards NF EN 13286-53 and NF P 98-114-3. To facilitate

**Table 4**  
Mechanical testing program.

Testing	Cure condition (Wet/Normal cure)	Dimension D × h (mm)	Number of replicates	Curing (days)
Normal proctor and IBI treatment ability (VS, ITS)	W at 40 °C	152x116 50x50	3, 3	7
UCS	N (endogenous) at 20 °C	50x100	3	14, 28, 56 and 90
UCS <sub>w</sub>	N (endogenous) at 20 °C, then, W at 20 °C	50x100	3	28 32
ITS	N (endogenous) at 20 °C	50 * 50	3	14, 28, 56 and 90

the volumetric swelling testing, the specimens were laterally covered with permeable textile bands and fixed with elastic bracelets. Conversely, for indirect tensile strength testing, impermeable film was used for lateral coverage. For each mix and each test, three replicates were prepared.

Before testing, the specimens were subjected to specific environmental conditions, first being placed in the air at a temperature of 20 °C and humidity of 90 %, and then immersed in water for 7 days at a temperature of 40 °C. Table 5 provides a summary of the treatment suitability criteria. A soil mix is deemed suitable if it meets the following requirements: 1) the volumetric swelling (VS) is below 5 % and 2) the indirect tensile strength (ITS) is greater than 0.2 MPa.

### 3.2.2.1. Short term mechanical properties

3.2.2.1.1. *Unconfined compressive strength (UCS)*. The trafficability criterion is determined by the circulation allowance age on a treated subgrade layer. To assess this criterion, unconfined compressive tests were conducted. Cylindrical specimens with a diameter (D) of 50 mm and a depth (H) of 100 mm were prepared using OWC and  $\rho = 0.985\rho_{\text{dopn}}$ . These specimens were then hermetically sealed in plastic molds to avoid moisture loss from the sample [51] and cured for 14, 28, 56, and 90 days at a temperature of 20 °C.

It is worth noting that the trafficability criterion, as defined by the French guide GTS [50], is met when the unconfined compressive strength exceeds 1 MPa.

3.2.2.1.2. *Resistance to wetting (UCS<sub>w</sub>)*. The specimens underwent an initial curing process in a climate-controlled room at a temperature of 20 °C, during which they were covered with impermeable film. This phase is referred to as the "normal cure." After 28 days, the plastic films were removed from the specimens. Subsequently, they were submerged in a container filled with water at the same temperature (20 °C) for an additional 32 days.

To evaluate the water sensitivity of the mix, the ratio UCS<sub>I60</sub> / UCS<sub>60</sub> was employed as a key metric.

3.2.2.1.3. *Resistance to freezing (ITS)*. The investigation into the resistance to freezing involved the use of indirect tensile tests. Cylindrical specimens, measuring 50 mm in diameter (D) and 50 mm in depth (H), were meticulously prepared using OWC and  $\rho = 0.96\rho_{\text{d}}$ , in accordance with NF EN 13286–53 standards. Subsequently, the specimens were hermetically sealed in plastic molds and stored in a climate-controlled room at a constant temperature of 20 °C for varying durations of 14, 28, 56, and 90 days.

The tensile strengths of the specimens were calculated using the following equation:

$$TS = 0.8 \times ITS \quad (1)$$

Where TS represents the estimated tensile strength derived from the ITS (MPa), and ITS denotes the Indirect Tensile Strength (MPa).

3.2.2.2. *Long term properties*. The indirect tensile strengths and elastic moduli were determined after 90 curing days. The estimated parameters (TS, E) after 360 curing days were then determined using empirical coefficients, which can be obtained using Eqs. (2) and (3) (NF P98–114–2).

$$\frac{R_t}{R_{t360}} = 0.70 \quad (2)$$

$$\frac{E_t}{E_{t360}} = 0.75 \quad (3)$$

The obtained tensile strengths and elastic moduli were then evaluated according to the Table 4 strength classes and defined in the standard NF P94–102–1 and the French technical guide GTR. The materials with a strength class lower than T4 cannot be used in road subgrade construction according to the specifications of the French standard NF P94–102–1.

### 3.2.3. Environmental assessment

The environmental impacts of the raw sediments were assessed through leaching tests, following the French standard NF EN 12457–2. The analysis was conducted on samples with a particle size of 4 mm and a liquid-solid ratio (L/S) of 10. Ion chromatography (IC) was employed to measure the concentrations of chloride, fluoride, and sulphate anions, while inductively coupled plasma-optical emission spectrometry (ICP) was used to measure the concentration of trace metals. The results presented in Table 7 indicate that the sediment concentrations of trace elements and anions are lower than those reported in the French SETRA guide [52]. Consequently, it can be inferred that the sediments are environmentally suitable for road subgrade construction.

**Table 5**  
Treated soil suitability evaluation criteria.

Soil treatment suitability assessment criteria	Parameters	
	VS (%)	ITS (MPa)
Suitable soil	≤ 5	≥ 0,2
Doubtful soil	5 ≤ VS ≤ 10	0,1 ≤ ITS ≤ 0,2
Unsuitable soil	≥ 10	≤ 0,1



**Table 6**  
Soil Long-term mechanical performance classification.

Position in the chart	Zone 1	Zone 2	Zone 3	Zone 4	Zone 5
Mechanical performance class	Class1	Class2	Class3	Class4	Class 5

**Table 7**  
Sediment road construction uses environmental acceptability criteria.

Elements	Raw Sediment (mg/kg of Dry Matter)	Inert Waste Reference (mg/kg of Dry Matter)	Thresholds SETRA for Alternative Materials
As	< 0.11	0.50	2.00
Ba	0.57	20.00	100.00
Cd	< 0.009	0.04	1.00
Cr	< 0.004	0.50	10.00
Cu	0.064	2.00	50.00
Mo	< 0.088	0.50	10.00
Ni	< 0.047	0.40	10.00
Pb	< 0.023	0.50	10.00
Sb	< 0.057	0.06	0.70
Se	< 0.083	0.10	0.50
Zn	0.02	4.00	50.00
Chloride	39.5	800.00	15,000.00
Fluoride	7.15	10.00	150.00
Sulfate	515	1000.00	20,000.00
Soluble fraction	1000	4000.00	60,000.00

## 4. Results and discussion

### 4.1. Dam sediment granular skeleton and binder dosage optimization

#### 4.1.1. Granular correction

As shown in Fig. 5, the mixes consisting of 60 % (or 70 %) of sandy marble waste (MW) and 40 % (or 30 %) of sediments (SED) belong to the optimal Fuller spindle. However, the mix composed of 50 % MW and 50 % SED, which is partially inside the T-F-T spindle, was selected to be treated herein by ternary binders to allow a maximum waste valorization.

Table 8 presents a concise summary of the physical properties pertaining to the 50 % SED + 50 % MW mixtures. The findings indicate that the introduction of marble waste has led to slight modifications in the geotechnical properties of the mixes. The treated sediments are categorized under class A3 F11 according to the GTR classification and the French standard NF P 11–300. Additionally, the inclusion of marble waste brings about changes in the granular skeleton of the mix, which in turn induces a dilution effect by altering the physical and geotechnical properties of the sediments [53].

4.1.1.1. Lime fixation point (LFP) and binder dosage. Fig. 6 provides a comprehensive overview of the mix suspension pH evolution

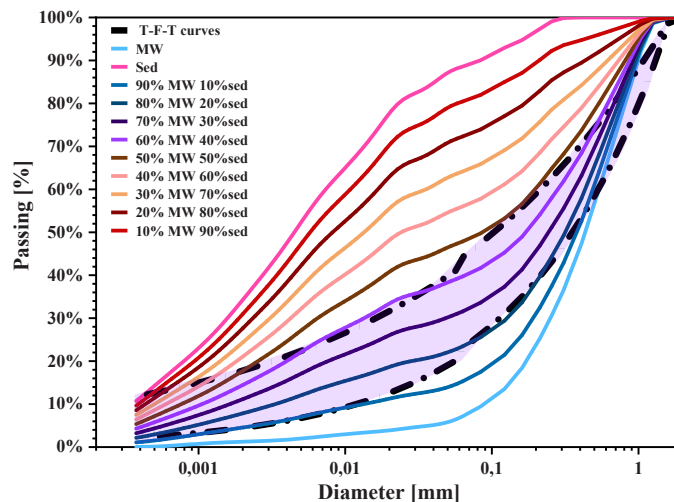


Fig. 5. Particle grain size distribution of the different Mix.

**Table 8**  
Mix 50 % SED + 50 % MW physical properties.

Properties	Test standards	50 % SED + 50 % MW
Laser granulometric analysis (Wet method):	ISO 13320-1	
Fine particles (% < 80 $\mu\text{m}$ )		49
Clayey fraction $D_{\text{max}} < 2 \mu\text{m}$ (%)		19.5
Silty fraction $2 \mu\text{m} < D_{\text{max}} < 63 \mu\text{m}$ (%)		28.5
Sandy fraction $63 \mu\text{m} < D < 2 \text{mm}$ (%)		52
Absolute density ( $\text{g}/\text{cm}^3$ )	NF EN 1097-7	2.67
Organic matter content at 450 °C	XP P 94-047	2.72
Loss on ignition at 550 °C	NF EN 15169	4.07
Blue methylene value ( $\text{g}/100 \text{g}$ )	NF P 94-068	3.92
Liquid limit (%)	NF P94-051	40.47
Plastic limit (%)	NF P94-051	13.75
Plasticity index (%)		27.22
Leaching test	EN 12457-2	Inert (French Directive of 14 December 2014)
Class	SETRA-LCPC	A <sub>3</sub> F <sub>11</sub>

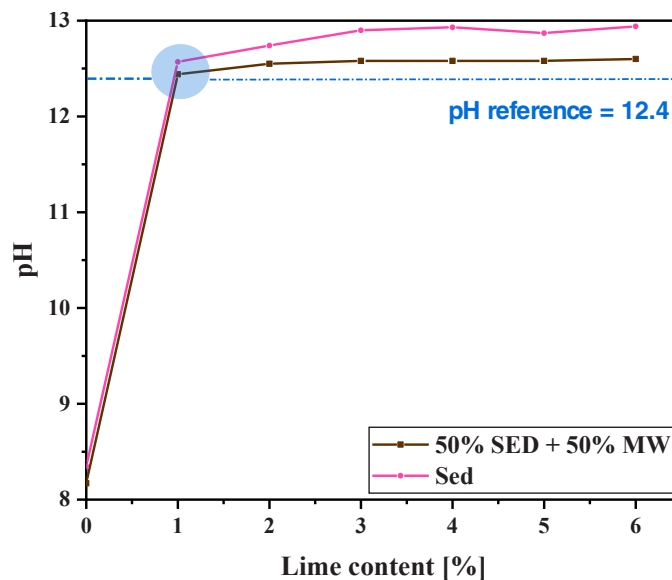


Fig. 6. pH variation as function of incorporated lime percentage.

concerning varying lime content. Notably, the mix suspension pH reached a critical value that marks the initiation of a pozzolanic reaction [54] when the sediment lime content reached 1 %. This observation suggests that the sediments exhibited a satisfactory affinity for lime and displayed an absorbed calcium saturation [10].

Over the long term, the hydration of lime leads to the production of calcium hydroxides, which subsequently react with aluminosilicate clay minerals, resulting in the formation of new hydration products. The rise in pH due to lime saturation significantly contributes to this reaction [55]. For this study, the lime content was consistently set at 1 % of the treated material's dry mass.

To effectively treat the Zardezdas dam sediments, which belong to class A3, a mixed treatment involving hydraulic binders and aerial lime is recommended, following the guidelines outlined in the French GTS guide. For the experimental investigation, two hydraulic

**Table 9**  
Mix design mixes.

Mix	S7-1	S7-2	S10-1	S10-2	SS7-1	SS7-2	SS10-1	SS10-2
Sediments	100 %	100 %	100 %	100 %	50 %	50 %	50 %	50 %
Sandy marble waste	0 %	0 %	0 %	0 %	50 %	50 %	50 %	50 %
Lime	1 %	1 %	1 %	1 %	1 %	1 %	1 %	1 %
HRB-1	7 %	0 %	10 %	0 %	7 %	0 %	10 %	0 %
HRB-2	0 %	7 %	0 %	10 %	0 %	7 %	0 %	10 %

road binder rates of 7 % and 10 % were selected based on the dry sediment weight. Detailed information regarding the composition of the investigated mixes can be found in Table 6.

## 4.2. Mechanical properties

### 4.2.1. Proctor test and IBI

Table 9 summarizes for each mix the optimum water content ( $w_{opt}$ ), the maximum dry density ( $\rho_d$ ) for each treatment, and the Immediate Bearing Index (IBI). The optimum moisture content  $W_{opt}$  has decreased from 19 % to 16.7 % for treated sediments and from 12.6 % to 14.7 % for 50 % MW mixes. On the other hand, the dry density  $\rho_d$  has increased especially for 50 % MW mixes. The dry densities ranged between 1.62 and 1.65 Mg/m<sup>3</sup> for treated sediments and between 1.93 and 1.96 Mg/m<sup>3</sup> for 50 % MW mixes. This may be due to the influence of binders and to the addition of the granulometric corrector, which has reduced the voids and improved the mix packing densities [56–58]. Fleureau et al. [59] has reported that the soil optimum Proctor depends on the liquid limit, which is confirmed by the fact that the raw sediment liquidity limit (52.10 %) was larger than that of the 50 % Sed+ 50 % MW mix (40.47 %).

The obtained mix IBI values ranged from 10.04 to 25.09, which satisfied the GTS guide requirements for use in road subgrades [50]. These results are in agreement with those reported in previous studies on treated sediments [8,60]. ( Table 10).

### 4.2.2. Treatment ability

Fig. 7 presents a summary of the volume swelling and indirect tensile strength characteristics. The results indicate that an increase in cement substitution rate with calcined sediments and LHF has led to a reduction in volumetric swelling. This observation could be attributed to the higher cement sulfate (SO<sub>3</sub>) content (approximately 4.09 %) compared to that in LHF (about 1.56 %) and calcined sediments (traces). This higher sulfate content might be responsible for the formation of ettringite.

Moreover, the mixes comprising 50 % marble sand and 50 % sediment experienced lower volumetric swelling in comparison to those consisting solely of treated raw sediments. This difference can be attributed to the higher liquid limit of the sediments (approximately 52.1 %) compared to that of the 50 %–50 % mixes (about 40.47 %). The presence of water creates a film on the particle surface, leading to volumetric swelling due to the high fine content in the 50–50 % mix [61]. Fleureau et al. [59] have reported that the volumetric swelling of mixes is directly proportional to their liquid limit and intragranular porosity.

However, the HRB Treatment alone does not achieve acceptable volumetric swelling thresholds for road subgrade layers [61]. Additionally, pyrite oxidation alters the mineralogical composition of the sediment and releases sulphate ions [62], particularly in an alkaline environment influenced by various factors such as pH, curing conditions, and physical characteristics of the sample [63]. In fact, the combination of sulphates with primary ettringite already present or C-A-H (produced by the binder hydration) enables the formation of additional ettringite [62] (as illustrated in Fig. 8). This phenomenon causes the appearance of cracks and deterioration of the sample [8].

Fig. 9 displays the correlation between VS and ITS for assessing treatment suitability criteria. The mixes SS7–1, SS7–2, and SS10–2, with volumetric swelling below the 5 % threshold, meet the criteria for indirect traction. Therefore, these mixes are the only ones considered suitable for treatment. The remaining mixes raise doubts regarding the effectiveness of lime and hydraulic road binder treatment.

### 4.2.2.1. Short term mechanical properties

4.2.2.1.1. *Unconfined compressive strength (UCS)*. Fig. 9 presents the compressive strength histograms of the different mixes after 14, 28, 56, and 90 days of curing. The reported compressive strength values are the averages of two specimen measurements. Notably, the strengths of most mixes showed an increase after 14 and 28 days, except for S10–2. Specifically, the treated sediments and 50 % Sed + 50 % MW mixes exhibited strength improvements from 1.11 to 2.12 MPa and from 1.95 to 3.95 MPa, respectively. These enhancements can be attributed to the production of C-A-S-H hydrates resulting from binder hydration and chemical reactions between the sediments and binders [64]. Additionally, intragranular void filling contributed to the observed strength increase.

It is worth noting that a slight strength decrease was observed between 28 and 56 days, except for the mixes SS7–2 and SS10–1. This decrease can be attributed to the influence of chemical compounds and sediment organic matter on the binder setting kinetics [8,15]. However, between 28 and 90 days, the compressive strengths of all treated mixes demonstrated growth resumption and further improvement. This ongoing strength enhancement is linked to continued new hydrate formations through pozzolanic reactions (slower than cement reaction), leading to a dense matrix with low porosity. This is clearly seen in the total porosity measurements at 28 and 90

**Table 10**  
Mix densification and bearing capacity parameters.

Mix	$\rho_d$ (Mg/m <sup>3</sup> )	$W_{OPN}$ (%)	IBI index
S7–1	1.64	18.50	18.73
S7–2	1.62	18.70	14.23
S10–1	1.63	19.00	16.46
S10–2	1.65	16.70	10.04
SS7–1	1.95	14.70	18.73
SS7–2	1.96	14.20	15.73
SS10–1	1.93	12.60	25.09
SS10–2	1.94	13.00	22.47

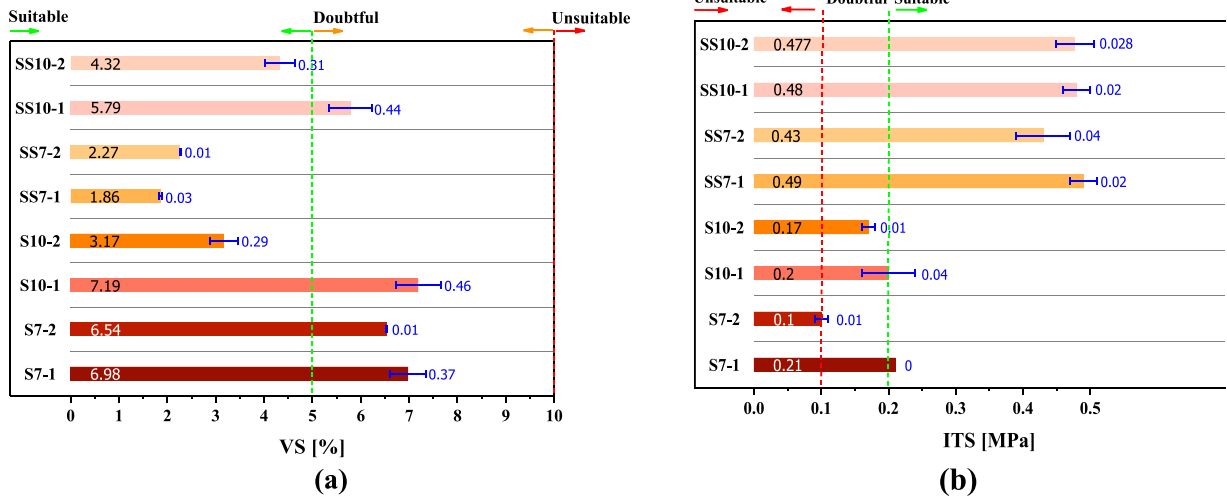


Fig. 7. (a) volumetric swelling and (b) indirect tensile strength measured after 7 days of water immersion in special conditions.

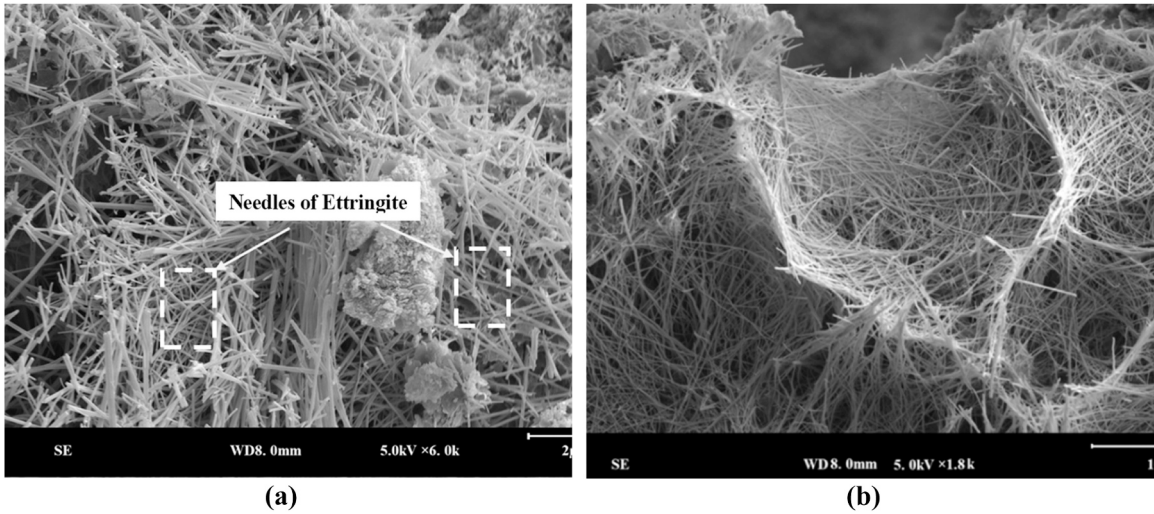


Fig. 8. Mix SEM observations (a) S7-1 and (b) S10-1 (SE mode).

days, which are reduced by around 20 % in formulations containing marble waste and sediment, compared with formulations containing only dam sediments (Table 11). The reaction of portlandite ( $\text{Ca}(\text{OH})_2$ ), released during cement hydration, with the reactive aluminosilicates phases of GGBS and calcined sediments (derived from the composition of HRB), forms additional C-S-H and strengthening. In addition, the increase in strength can be also attributed to the formation of these C-S-H and C-A-H from the reaction between the Zardezas clayey sediments and hydrated lime. Upon introducing hydrated lime to the sediments, it dissociates into calcium ions ( $\text{Ca}^{2+}$ ) and hydroxide ions ( $\text{OH}^-$ ). The release of hydroxide ions increases the soil pH, the pH is raised to 12.4. The high pH led to the dissolution of silica ( $\text{SiO}_2$ ) and alumina ( $\text{Al}_2\text{O}_3$ ) from clay minerals present in the sediments. The dissolved silica and alumina react with calcium ions in the soil solution to form calcium-silicate-hydrates (C-S-H) and calcium-aluminate-hydrates (C-A-H). This corresponds to research conducted on stabilized soils [12,51,55,65].

Furthermore, the compressive strengths of the 50 % Sed + 50 % MW mixes consistently outperformed those of the treated sediment mixes, irrespective of the curing duration and binder content. For example, the SS10-1 mix exhibited twice the compressive strength of the S10-1 mix. Similar results were reported by Boutouil et al. [45] and Maherzi et al. [8] when improving the sediment particle sizes by adding sand as a granular corrector at various proportions (Table 11).

After only 14 curing days, all mixes surpassed the minimum trafficability criteria of 1 MPa required for road sublayer use. Notably, according to the specifications of the GTS guide [50], all mixes met the circulation age requirement after 14 days of curing. Additionally, it is possible to estimate the minimum age required to achieve subgrade layer trafficability criteria using the 7-day compressive strengths. (Fig. 10).

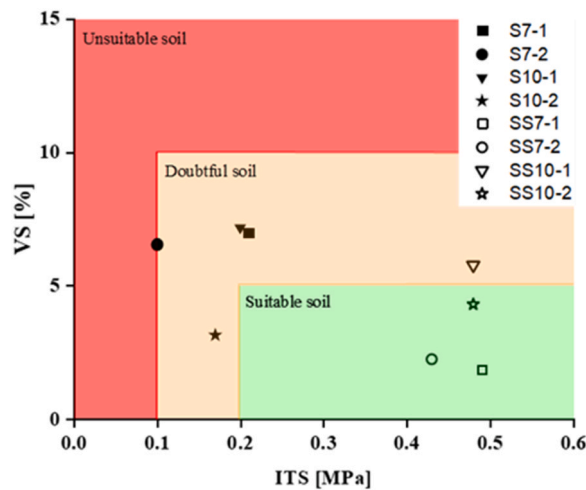


Fig. 9. ITS and VS correlation of the different mixtures.

Table 11

Evolution of the total porosity of the different mixtures.

Mix	28 days	90 days
S7-1	32.50 %	32.55 %
S7-2	32.44 %	32.00 %
S10-1	31.92 %	32.29 %
S10-2	32.11 %	33.75 %
SS7-1	25.51 %	25.27 %
SS7-2	26.48 %	26.49 %
SS10-1	26.30 %	22.64 %
SS10-2	26.46 %	22.67 %

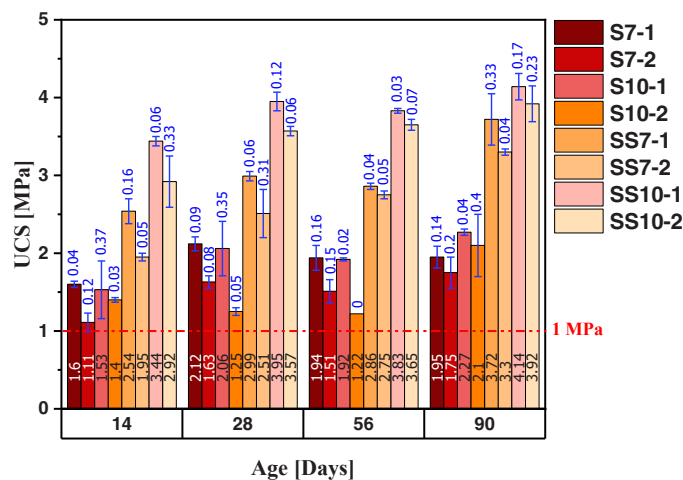


Fig. 10. Evolution of unconfined compressive strength over time based on treatment type.

Fig. 11-a illustrates the influence of granular corrector and packing density on the mechanical properties of the investigated mixtures. It was observed that granular mixes with higher compactness exhibited the most favorable mechanical performance across various curing periods. This finding aligns with previously reported results [8,9,40,46,60].

Furthermore, Fig. 11-b reveals that the strength gains of HRB-2 mixes were more important compared with those of HRB-1 batches. These results could be attributed to the distinct chemical composition of the hydraulic road binders used. Specifically, the CaO/SiO<sub>2</sub> ratio was found to be 2.38 for HRB-1 and 1.62 for HRB-2, respectively. Notably, these results are consistent with earlier studies, which have indicated that the optimal binder performance typically corresponds to a ratio of around 1.7 [8].

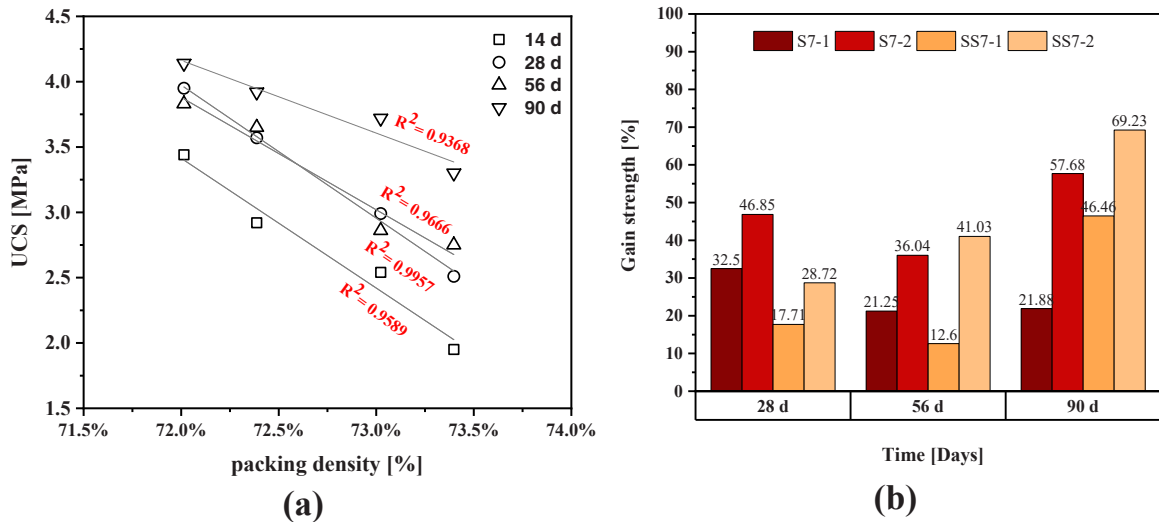


Fig. 11. Physical and chemical treatment impacts on mix strength gains.

4.2.2.1.2. *Resistance to wetting (UCSI)*. Table 12 shows early age immersion test results after 28 normal curing days and 32 water immersion days. The table values represent the average of two specimen measurements. The results show that the strength of the specimens after water immersion are lower than those of the specimens after normal curing. This decrease may be caused by water penetration in the pores. The early age immersion of all mixes exceeds the lower threshold limit of 0.6 (MBV  $\geq$  0.5 g/100 g), which is specified by the GTS guide [50]. The resistance to wetting criteria was therefore satisfied and all the mixes did not show any water sensitivity. These findings are similar to those reported in prior studies [60].

4.2.2.1.3. *Resistance to freezing (indirect tensile test (ITS))*. The results represent the average of two specimen measurements. Fig. 12 shows the mix indirect tensile strength results. On the 14th and 28th days, the indirect tensile strengths decreased for all mixes especially those with sediments and binder treated. After the 28th day, the indirect tensile strength increased for all mixes, except for the sediment-only ones which remained more or less stable at the 90th day.

It is worth noting that 50 %Sed + 50 % MW mixes have developed a frost resistance between 0.35 and 0.42 MPa, which meets GTS [50] requirements (Rit  $\geq$  0.25 MPa). This finding is in accordance with that reported by Boutouil et al. [45] and Kasmi et al. [56] on granular corrector impacts on mix mechanical properties. For treated sediment mixes, the S10–1, S7–1, and S10–2 mixes reached the threshold value of 0.25 MPa after 90, 28, and 56 curing days, respectively. However, the S7–2 mix did not reach the threshold value for all ages.

4.2.2.2. *Long term mechanical properties*. A suitable subgrade material must be classified at least a resistance class 4 according to the standard NF P94–102–1.

The classification diagram according to the couple (Rt, E) shows that all the formulations are classified beyond Zone 5, except the S10–1 formulation, which is in zone 5. (Fig.13).

The two formulations SS10–2 and SS7–1 are in zone 2 corresponding to the mechanical class 2 followed by S7–1, S7–2 and SS10–1 in zone 3 (mechanical class 3), S10–2 and SS7–2 in zone 4 (mechanical strength class 4). All the formulations meet the requirements of the standard NF P94–102–1 for use in subgrade according to the long-term mechanical class, determined according to of the couple (Rt, E).

Table 12  
UCSI and UCS after 28 normal curing days and 32 immersion days.

Mixtures	UCSI (MPa)	Standard deviation	UCS (MPa)	UCSI/UCS
S7–1	1.41	0.23	1.94	0.73
S7–2	1.19	0.11	1.51	0.79
S10–1	1.63	0.02	1.92	0.85
S10–2	0.76	2.13	1.22	0.62
SS7–1	2.13	0.24	2.86	0.75
SS7–2	2.51	0.03	2.75	0.91
SS10–1	2.27	0.09	3.83	0.70
SS10–2	2.51	0.23	3.65	0.60



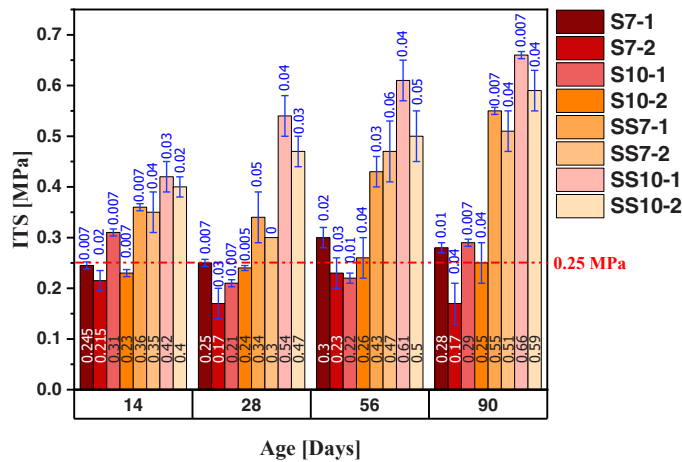


Fig. 12. Mix indirect tensile strengths.

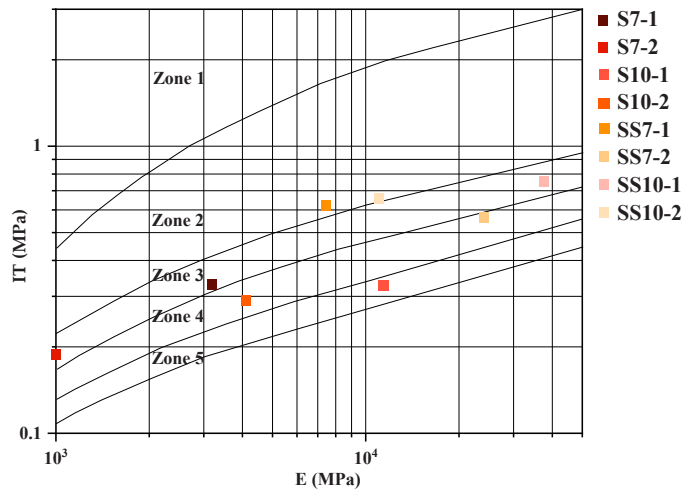


Fig. 13. Mix mechanical strength classes according to long-term criteria ( $E$ ,  $R_f$ ).

4.3. Mix environmental assessments

The environmental impacts of the mixes were assessed after 28 curing days using batch leaching according to the standard NF EN 12457–2. The obtained concentration results did not exceed the threshold limits specified by the SETRA guide [52]. All of the mixes complied with the environmental requirements for use on road subgrades.

4.4. Greenhouse gas effect and energy consumption

The construction industry faces a critical challenge in curbing its environmental impact through the reduction of energy consumption and the sustainable extraction of natural resources. Notably, the production of aggregates plays a significant role in this impact, as it accounts for approximately 32 kg CO<sub>2</sub> eq/t [66]. Additionally, it is essential to underscore that the transportation of aggregates from the quarry to the construction site is responsible for about 5 % of the overall Global Warming Potential (GWP) (see Table 12).

A life cycle analysis was undertaken to evaluate the environmental advantages, global warming potential, and energy consumption associated with both natural and recycled sand derived from a blend of sediments and marble waste. The methodology employed for this assessment is illustrated in Fig. 14. The study focused on a sand production quarry located in Skikda, which the annual production is estimated at around 96,000 tons per year.

In the first scenario, the study focused on the environmental impact of the production of approximately 19,200 tons per year of crushed sand (20 % of the total sand production). In contrast, the second scenario explored the utilization of 20 % recycled sand as a replacement for the crushed sand. Specifically, this alternative scenario yielded an output of approximately 19,200 tons of natural

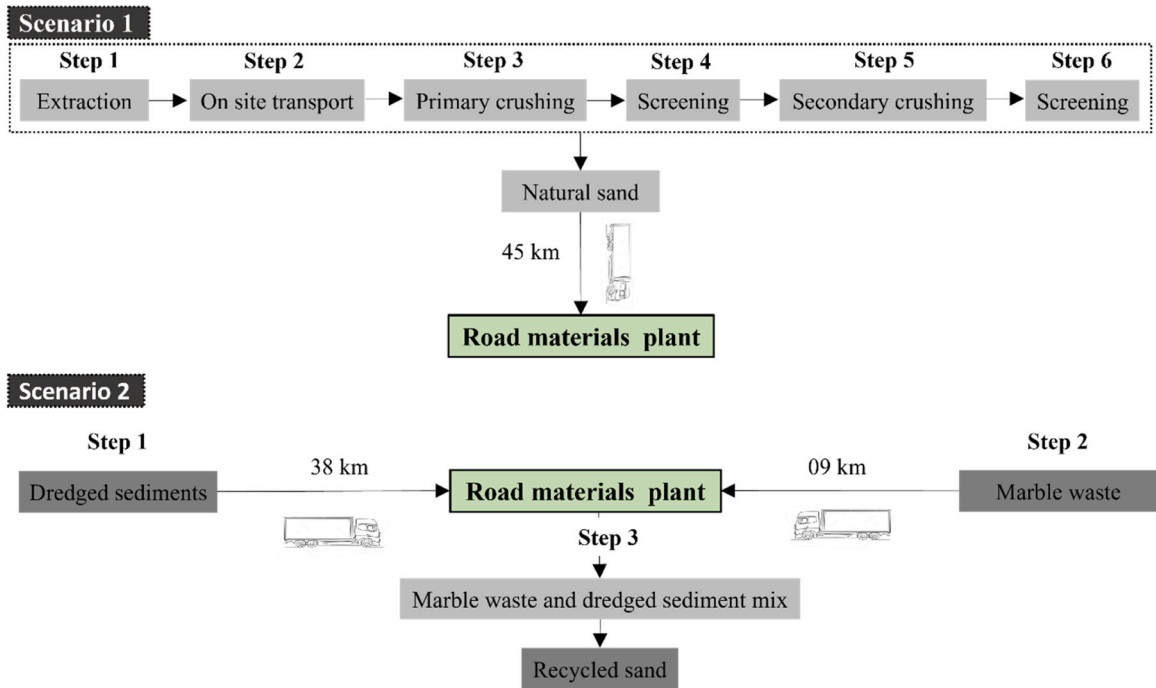


Fig. 14. Marble waste and dredged sediment mix production scenarios (the light gray boxes represent the stages considered in the LCA).

sand, achieved through the incorporation of the recycled sand.

It is essential to highlight the significance of these findings as they shed light on the potential environmental benefits of incorporating recycled sand into the production process, thereby reducing the demand for natural sand extraction and its associated environmental impacts.

The materials are anticipated to undergo mixing at a plant situated in close proximity to both the natural sand quarry (45 km away) and the recycled sand quarry (47 km away). Transportation of the natural and recycled sands between different production and processing units is envisaged to occur via trucks with a storage capacity of 40 tons per trip. Notably, the study focuses solely on the transportation and loading processes of marble waste and raw sediment, as they fall under the category of solid waste.

The global warming potential and energy consumption were assessed based on data from previously published studies [71–73]. For the determination of transportation energy, we relied on the average fuel consumption of a 40-ton truck carrying a standard load [74]. The detailed calculations can be found in Table 13 and Table 14. (, Tables 15 and 16).

Fig. 15 clearly illustrates the substantial impact of integrating 20 % recycled sand in place of natural sand, resulting in a significant reduction of approximately 28 % in annual CO<sub>2</sub> emissions. This reduction can be attributed to the more efficient handling and transportation process associated with the use of recycled sands, limited only to the phases of stock handling and transport from waste storage areas to the mix production plant. Moreover, the adoption of recycled sand leads to a noteworthy decrease of approximately 44

Table 13  
Leaching test results of studied mixes.

Elements	Raw Sed	S7-1	S7-2	S10-1	S10-2	SS7-1	SS7-2	SS10-1	SS10-2	SETRA thresholds
As	< 0.11	< 0.10	< 0.10	< 0.10	< 0.10	< 0.10	< 0.10	< 0.10	< 0.10	1.500
Ba	0.57	0.691	0.690	1.403	1.305	1.982	3.121	4.957	5.030	60.000
Cd	< 0.009	< 0.009	< 0.009	< 0.009	< 0.009	< 0.009	< 0.009	< 0.009	< 0.009	0.120
Cr	< 0.004	0.669	0.540	1.173	0.684	0.586	0.496	0.329	0.449	1.500
Cu	0.064	1.292	1.133	0.838	1.232	0.773	0.741	0.575	0.629	6.000
Mo	< 0.088	0.238	0.227	0.223	0.247	0.126	0.161	< 0.090	0.154	1.500
Ni	< 0.047	0.277	0.196	0.263	0.246	0.256	0.196	0.222	0.170	1.200
Pb	< 0.023	< 0.030	< 0.030	< 0.030	< 0.030	< 0.030	< 0.030	< 0.030	< 0.030	1.500
Sb	< 0.057	< 0.060	< 0.060	< 0.060	< 0.060	< 0.060	< 0.060	< 0.060	< 0.060	0.180
Se	< 0.083	< 0.080	< 0.080	< 0.080	< 0.080	< 0.080	< 0.080	< 0.080	< 0.080	0.300
Zn	0.02	< 0.010	0.016	0.026	0.014	< 0.010	0.017	0.015	0.012	12.000
Fluoride	39.5	11	13	11	12	7	7	7	9	30
Chloride	7.15	65	59	74	66	28	27	33	37	2400
Sulfate	515	760	810	330	870	260	260	670	120	3000

**Table 14**  
Public sand production GWP and energy consumption values.

	GWP [kg CO <sub>2</sub> eq/t]	Energie, fossil fuels [MJ/t]	Reference
Natural sand production	2.51–11.4	61.89–110	[67–71]
Transportation	0.14 (truck transport 35 t)	2.04	[69,71]
Front end loader	0.7	10.41	[71]

**Table 15**  
Natural and recycled sand global warming potential determination.

Production Process Activities	Sand quantity production	Climate change	
		Natural sand production	Recycled Sand
<b>Production [kg eq. CO<sub>2</sub>/t]</b>		Extraction/Loading (5 km)/crushing/washing/ screening)	Front end loader
	1 ton	2.6	0.7
	19,200 tons	49,920	13,440
<b>Transportation [kg eq. CO<sub>2</sub>/t]</b>	1 ton	3.51 (45 km)	3.66 (47 km)
	19,200 tons	67,392	70,272
<b>Total [kg eq. CO<sub>2</sub>/t]</b>	1 ton	6.11	4.36
	19,200 tons	<b>117,312</b>	<b>83,712</b>
<b>Total CO<sub>2</sub> prevented [kg eq. CO<sub>2</sub>/year]</b>	<b>19,200 tons</b>	<b>33,600</b>	

**Table 16**  
Natural and recycled sand energy consumption.

Production Process Activities	Sand quantity production	Energy consumption	
		Natural sand production	Recycled Sand
<b>Production [MJ/t]</b>		Extraction/Loading (5 km)/crushing/washing/ screening)	Front end loader
	1 ton	33.80	10.41
	19,200 tons	648,960	199,872
<b>Transportation [MJ/t]</b>	1 ton	17.55 (45 km)	18.33 (47 km)
	19,200 tons	336,960	351,936
<b>Total energy consumption [MJ/year]</b>	1 ton	51.35	28.74
	19,200 tons	<b>985,920</b>	<b>551,808</b>
<b>Total energy consumption prevented [MJ/year]</b>	<b>19,200 tons</b>	<b>434,112</b>	

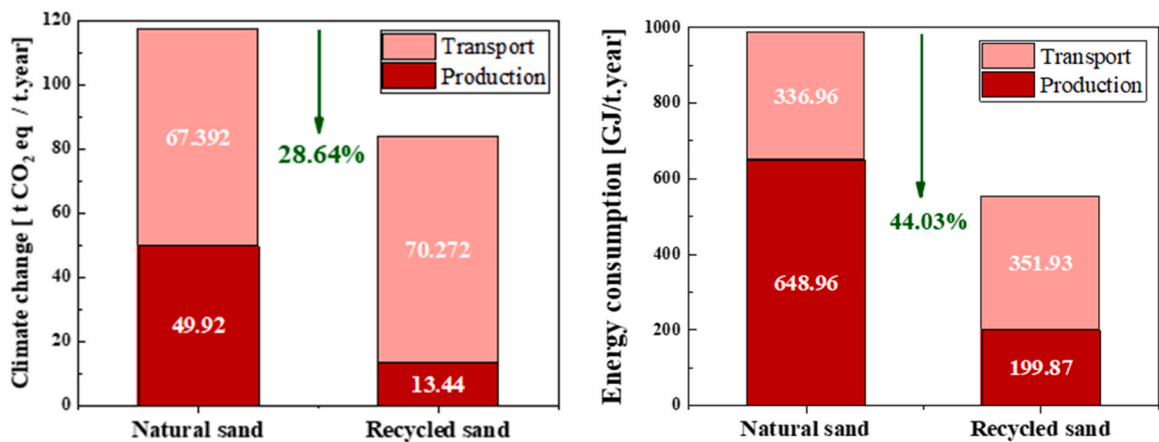


Fig. 15. Sand production scenario greenhouse gas effect and energy consumption.

% in energy consumption when compared to the production of natural sand. Indeed, replacing 20 % of natural sand, allows us to avoid extracting 19,200 t of natural sand per year, and consequently extends the quarry's lifespan by about 25 years.

## 5. Conclusions

The present study aimed to assess the feasibility of using Zardezas dam sediments in road subgrade construction after undergoing various treatments. The composition of the 50 % sediment + 50 % marble waste mixture was optimized using the optimal spindle defined by the Talbot-Fuller-Thompson reference curves. Subsequently, eight different mixes, with and without granular corrector, were treated with lime and hydraulic road binders, in accordance with the recommendations of the French GTS guide. The following conclusions can be highlighted:

- The addition of marble waste has enhanced the granular structure of the sediments. The evaluation of treatment effects was based on an analysis of short and long-term mechanical properties and microstructural changes. After treatment with hydraulic binders and lime, only the SS7-1, SS7-2 and SS10-2 mixes achieved the desired performance for road sub-base applications. This result was attributed to the beneficial contribution of marble waste, which improved packing density and porosity.
- All the mixes showed satisfactory compressive strengths after 14 days. In addition, their wetting resistance proved satisfactory in relation to the criteria specified in the French guide for road construction. In particular, mixes composed of 50 % sediment and 50 % marble sand showed satisfactory frost resistance after only 14 days curing. This is demonstrated by SEM images showing a less porous structure and lower sulfate expansion products.
- The results of this study highlighted the importance of the choice of hydraulic binder for the treatment of mixes. In fact, a hydraulic road binder with a CaO/SiO<sub>2</sub> ratio of around 1.70 is highly recommended to achieve the desired performance.
- Based on an assessment of mechanical strength classes (Rt, E) and environmental factors, it is apparent that only mixes SS7-1, SS7-2, and SS10-2 are deemed suitable for application in road subgrade construction.
- Lastly, with regards to the Algerian region of Skikda, adopting a yearly utilization of 20 % natural and recycled sand could potentially lead to a substantial reduction of greenhouse gas emissions by approximately 30 % and fossil fuel consumption by over 40 %. This highlights the environmental benefits associated with incorporating sustainable practices in road construction.

In conclusion, the comprehensive evaluation conducted in this study provides valuable insights into the use of Zardezas dam sediments in road subgrade construction, identifying the most suitable mixes and emphasizing the significance of sustainable materials in reducing environmental impacts.

## CRedit authorship contribution statement

**Salim Mezazigh:** Funding acquisition, Investigation, Methodology, Project administration, Resources, Supervision, Validation, Visualization, Writing – review & editing. **Walid Maherzi:** Conceptualization, Data curation, Funding acquisition, Investigation, Methodology, Resources, Supervision, Validation, Visualization, Writing – review & editing. **Ahmed Senouci:** Methodology, Validation, Visualization, Writing – review & editing. **Selma Bellara:** Data curation, Formal analysis, Investigation, Methodology, Resources, Writing – original draft.

## Declaration of Competing Interest

This manuscript has not been published or presented elsewhere in part or in entirety and is not under consideration by another journal. We have read and understood your journal's policies, and we believe that neither the manuscript nor the study violates any of these. There are no conflicts of interest to declare.

## Data availability

No data was used for the research described in the article.

## References

- [1] A.P. Adebowale, O.A. Asa, O.J. Omotehinse, I.A. Ankeli, D.I. Dabara, The need for green building rating systems development for Nigeria: the process, progress and prospect, *Acad. J. Sci.* 07 (2019) 35–44.
- [2] Y.H. Labaran, V.S. Mathur, S.U. Muhammad, A.A. Musa, Carbon footprint management: a review of construction industry, *Clean. Eng. Technol.* 9 (2022), 100531, <https://doi.org/10.1016/j.clet.2022.100531>.
- [3] F. Hadji, N. Ihaddadene, R. Ihaddadene, A. Betga, A. Charick, P.O. Logerais, Thermal conductivity of two kinds of earthen building materials formerly used in Algeria, *J. Build. Eng.* 32 (2020), 101823, <https://doi.org/10.1016/j.job.2020.101823>.
- [4] E.K. Anastasiou, A. Liapis, I. Papayianni, Comparative life cycle assessment of concrete road pavements using industrial by-products as alternative materials, *Resour. Conserv. Recycl.* 101 (2015) 1–8, <https://doi.org/10.1016/j.resconrec.2015.05.009>.
- [5] S.I. Mohammed, K.B. Najim, Mechanical strength, flexural behavior and fracture energy of recycled concrete aggregate self-compacting concrete, *Structures* 23 (2020) 34–43, <https://doi.org/10.1016/j.istruc.2019.09.010>.
- [6] F. Hallouz, M. Meddi, G. Mahé, S. Toumi, S.E.A. Rahmani, Erosion, suspended sediment transport and sedimentation on the Wadi Mina at the Sidi M'Hamed Ben Aouda Dam, Algeria, *Water* 10 (2018), <https://doi.org/10.3390/w10070895>.

- [7] F. Baraud, L. Leleyter, S. Poree, T. Lecomte, Environmental availability of trace metals in a fired brick elaborated from a marine dredged sediment, *Environ. Sci. Pollut. Res.* (2023), <https://doi.org/10.1007/s11356-023-26163-6>.
- [8] W. Maherzi, M. Benzerzour, Y. Mamindy-Pajany, E. van Veen, M. Boutouil, N.E. Abriak, Beneficial reuse of Brest-Harbor (France)-dredged sediment as alternative material in road building: laboratory investigations, *Environ. Technol. (U. Kingd.)* 39 (2018) 566–580, <https://doi.org/10.1080/09593330.2017.1308440>.
- [9] S. Bellara, M. Hidjeb, W. Maherzi, S. Mezazigh, S. Ahmed, Optimization of an eco-friendly hydraulic road binders comprising clayey dam sediments and ground granulated, buildings 11 (2021) 443, <https://doi.org/10.3390/buildings11100443>.
- [10] W. Maherzi, F. Ben Abdelghani, Dredged marine raw sediments geotechnical characterization for their reuse in road construction, *Eng. J.* 18 (2014) 27–37, <https://doi.org/10.4186/ej.2014.18.4.27>.
- [11] T. Chompoorat, T. Maikhun, S. Likitlersuang, Cement-Improved Lake Bed sedimentary soil for road construction, *Proc. Inst. Civ. Eng. Gr. Improv.* 172 (2019) 192–201, <https://doi.org/10.1680/jgrim.18.00076>.
- [12] T. Chompoorat, K. Thanawong, S. Likitlersuang, Swell-shrink behaviour of cement with fly ash-stabilised lakebed sediment, *Bull. Eng. Geol. Environ.* 80 (2021) 2617–2628, <https://doi.org/10.1007/s10064-020-02069-2>.
- [13] S. Mkaour, W. Maherzi, P. Pizette, H. Zaitan, M. Benzina, A comparative study of natural Tunisian Clay types in the formulation of compacted earth blocks, *J. Afr. Earth Sci.* 160 (2019), 103620, <https://doi.org/10.1016/j.jafrearsci.2019.103620>.
- [14] A.N. Adazabra, G. Viruthagiri, J. Atingabono, Developing fired clay bricks by incorporating scrap incinerated waste and river dredged sediment, *Process Saf. Environ. Prot.* 179 (2023) 108–123, <https://doi.org/10.1016/j.psep.2023.08.078>.
- [15] H. Beddaa, I. Ouazi, A. Ben Fraj, F. Laverigne, J.M. Torrenti, Reuse potential of dredged river sediments in concrete: effect of sediment variability, *J. Clean. Prod.* 265 (2020), 121665, <https://doi.org/10.1016/j.jclepro.2020.121665>.
- [16] T. Soleimani, M. Hayek, G. Junqua, M. Salgues, J.-C. Souche, Environmental, economic and experimental assessment of the valorization of dredged sediment through sand substitution in concrete, *Sci. Total Environ.* 858 (2023), 159980, <https://doi.org/10.1016/j.scitotenv.2022.159980>.
- [17] W. Xu, Z. Song, M. Guo, L. Jiang, H. Chu, Improvement in water resistance of magnesium oxychloride cement via incorporation of dredged sediment, *J. Clean. Prod.* 356 (2022), 131830, <https://doi.org/10.1016/j.jclepro.2022.131830>.
- [18] R. Hadj Sadok, N. Belas, M. Tahlaoui, R. Mazouzi, Reusing calcined sediments from Chorfa II Dam as partial replacement of cement for sustainable mortar production, *J. Build. Eng.* 40 (2021), <https://doi.org/10.1016/j.jobee.2021.102273>.
- [19] E. Rozière, M. Samara, A. Loukili, D. Damidot, E. Rozière, M. Samara, A. Loukili, D. Damidot, Valorisation of Sediments in Self-Consolidating Concrete: Mix-Design and Microstructure., doi:10.1016/j.conbuildmat.2015.01.080f.
- [20] F. Taieb, N. Belas, H.A. Mesbah, Influence of treated mud on free shrinkage and cracking tendency of self-compacting concrete equivalent mortars, *Mater. Constr.* 69 (2019).
- [21] A. Bouchikhi, Y. Mamindy-Pajany, W. Maherzi, C. Albert-Mercier, H. El-Moueden, M. Benzerzour, A. Peys, N.E. Abriak, Use of residual waste glass in an alkali-activated binder – structural characterization, environmental leaching behavior and comparison of reactivity, *J. Build. Eng.* 34 (2021), 101903, <https://doi.org/10.1016/j.jobee.2020.101903>.
- [22] F. Belayali, W. Maherzi, M. Benzerzour, N.E. Abriak, A. Senouci, Compressed Earth blocks using sediments and alkali-activated byproducts, *Sustain* 14 (2022), <https://doi.org/10.3390/su14063158>.
- [23] F. Belayali, W. Maherzi, M. Benzerzour, N.-E. Abriak, Influence of the physical and chemical characteristics of sediment fillers on the properties of mastic asphalt, *Powder Technol.* 421 (2023), 118393, <https://doi.org/10.1016/j.powtec.2023.118393>.
- [24] G. Renella, Recycling and reuse of sediments in agriculture, *Where Is. Probl.?* (2021).
- [25] J. Limeira, M. Etxeberria, L. Agulló, D. Molina, Mechanical and durability properties of concrete made with dredged marine sand, *Constr. Build. Mater.* 25 (2011) 4165–4174, <https://doi.org/10.1016/j.conbuildmat.2011.04.053>.
- [26] J.J.J. Herrmann, D. Attanasio, R.H. Tykot, Aspects of the trade in colored marbles in Algeria, *L’Africa Rom.* 2 (2012) 1331–1342.
- [27] S. Papatzani, A review on the valorization of marble dust/solids or slurry: classification, current trends and potentials, *Indian Concr. J.* 93 (2019) 36–54.
- [28] Indian embassy algiers Monthly Commercial Report for the Month of February 2020; 2020;
- [29] N. Toubal Seghir, M. Mellas, L. Sadowski, A. Žak, Effects of marble powder on the properties of the air-cured blended cement paste, *J. Clean. Prod.* 183 (2018) 858–868, <https://doi.org/10.1016/j.jclepro.2018.01.267>.
- [30] N.W. Jassim, H.A. Hassan, H.A. Mohammed, M.Y. Fattah, Utilization of waste marble powder as sustainable stabilization materials for subgrade layer, *Results Eng.* 14 (2022), 100436, <https://doi.org/10.1016/j.rineng.2022.100436>.
- [31] A.K. Jain, A.K. Jha, Shivanshi, Geotechnical behaviour and micro-analyses of expansive soil amended with marble dust, *Soils Found.* 60 (2020) 737–751, <https://doi.org/10.1016/j.sandf.2020.02.013>.
- [32] H.A. El-Sayed, A.B. Farag, A.M. Kandeel, A.A. Younes, M.M. Yousef, Characteristics of the marble processing powder waste at Shaq El-Thoaban Industrial Area, Egypt, and Its Suitability for Cement Manufacture, *HBRC J.* 14 (2018) 171–179, <https://doi.org/10.1016/j.hbrj.2016.06.002>.
- [33] M. Monica, C. Dhoka, Green concrete: using industrial waste of marble powder, quarry dust and paper pulp, *Int. J. Eng. Sci. Invent.* 2 (2013) 67–70.
- [34] K. Vardhan, S. Goyal, R. Siddique, M. Singh, Mechanical properties and microstructural analysis of cement mortar incorporating marble powder as partial replacement of cement, *Constr. Build. Mater.* 96 (2015) 615–621, <https://doi.org/10.1016/j.conbuildmat.2015.08.071>.
- [35] Touni A.; Remini B. ZARDEZAS (ALGERIA): A DAM THAT IS SILTING UP? LARHYSS J. P-ISSN 1112-3680/E-ISSN 2521-9782 2020, 43, 181–196.
- [36] LCPC-SETRA Réalisation Des Remblais et Des Couches de Forme, Fascicule I 2000, 102.
- [37] A. Benaissa, Z. Aloui, S. Moulay Ghembaza, D. Levacher, Y. Sebaibi, Behavior of sediment from the dam FERGOUG in road construction, *Adv. Concr. Constr.* 4 (2016) 15–26.
- [38] B. Serbah, N. Abou-bekr, S. Bouchemella, J. Eid, S. Taibi, Dredged sediments valorisation in compressed earth blocks: suction and water content effect on their mechanical properties, *Constr. Build. Mater.* 158 (2018) 503–515, <https://doi.org/10.1016/j.conbuildmat.2017.10.043>.
- [39] B. Remini, Valorisation de La Vase Des Barrages Quelques Exemples Algériens, *Larhyss J.* 5 (2006) 75–89.
- [40] I. Ennahal, W. Maherzi, M. Benzerzour, Y. Mamindy, N.E. Abriak, Performance of lightweight aggregates comprised of sediments and thermoplastic waste, *Waste Biomass.-. Valoriz.* 12 (2021) 515–530, <https://doi.org/10.1007/s12649-020-00970-1>.
- [41] R. Snellings, Ö. Cizer, L. Horckmans, P.T. Durdziński, P. Dierckx, P. Nielsen, K. Van Balen, L. Vandewalle, Properties and pozzolanic reactivity of flash calcined dredging sediments, *Appl. Clay Sci.* 129 (2016) 35–39, <https://doi.org/10.1016/j.clay.2016.04.019>.
- [42] C. Van Bunderen, R. Snellings, L. Vandewalle, Ö. Cizer, Early-age hydration and autogenous deformation of cement paste containing flash calcined dredging sediments, *Constr. Build. Mater.* 200 (2019) 104–115, <https://doi.org/10.1016/j.conbuildmat.2018.12.090>.
- [43] T. Chompoorat, T. Thepumong, S. Taesinlapachai, S. Likitlersuang, Repurposing of stabilised dredged lakebed sediment in road base construction, *J. Soils Sediment.* 21 (2021) 2719–2730, <https://doi.org/10.1007/s11368-021-02974-3>.
- [44] D. Levacher, D. Colin, A.C. Perroni, Z. Duan, L. Sun, Recyclage et Valorisation de Sédiments Fins de Dragage à Usage de Matériaux Routiers, IXèmes Journ. Natl. Génie Civil–Génie Côtier, Fr. (2006), <https://doi.org/10.5150/jngcgc.2006.058-1>.
- [45] M. BOUTOUIL, L. SAUSSAYE, Influence de l’ajout d’un Correcteur Granulométrique Sur Les Propriétés Des Sédiments Traités Aux Liants Hydrauliques, *Rev. Paralia* 15 (2011) 229–238, <https://doi.org/10.5150/revue-paralia.2011.008>.
- [46] Z. Mkahal, Y. Mamindy-Pajany, W. Maherzi, N.E. Abriak, Recycling of mineral solid wastes in backfill road materials: technical and environmental investigations, *Waste Biomass.-. Valoriz.* 13 (2022) 667–687, <https://doi.org/10.1007/s12649-021-01544-5>.
- [47] B. Banoune, Comportement Mécanique et Durabilité Des Matériaux Routiers à Différents Dosages En Sédiments Fins, 2016.
- [48] J. Eades, R. Grim, A Quick Test to Determine Lime Requirements for Lime Stabilization. *Environ. Sci.* 1966.
- [49] A. al-Swaidani, I. Hammoud, A. Meziab, Effect of adding natural pozzolana on geotechnical properties of lime-stabilized clayey soil, *J. Rock. Mech. Geotech. Eng.* 8 (2016) 714–725, <https://doi.org/10.1016/j.jrmge.2016.04.002>.

- [50] LCPC-SETRA, *Traitement Des Sols à La Chaux et/Ou Aux Liants Hydrauliques. Application à La Réalisation Des Remblais et Des Couches de Forme*, Bull. Des. Lab. Des. Ponts Chauss. (2000) 240.
- [51] N. Yoobanpot, P. Jamsawang, P. Simarat, P. Jongpradist, S. Likitlersuang, Sustainable reuse of dredged sediments as pavement materials by cement and fly ash stabilization, *J. Soils Sediment.* 20 (2020) 3807–3823, <https://doi.org/10.1007/s11368-020-02635-x>.
- [52] SETRA, *Acceptabilité de Matériaux Alternatifs En Technique Routière - Evaluation Environnementale*, 2011.
- [53] E. Silitonga, *Valorisation Des Sédiments Marins Contaminés Par Solidification / Stabilisation à Base de Liants Hydrauliques et de Fumée de Silice*, Université de Caen Normandie, 2010.
- [54] I. Djeran-Maigre, A. Morsel, L. Briançon, E. Delfosse, D. Levacher, A.R. Razakamanantsoa, Uses of usumacinta river sediments as a sustainable resource for unpaved roads: an experimental study on a full-scale pilot unit, *Transp. Eng.* 9 (2022), 100136, <https://doi.org/10.1016/j.treng.2022.100136>.
- [55] P. Akula, D.N. Little, Analytical tests to evaluate pozzolanic reaction in lime stabilized soils, *MethodsX* 7 (2020), <https://doi.org/10.1016/j.mex.2020.100928>.
- [56] A. Kasmi, N.E. Abriak, M. Benzerzour, H. Azrar, Environmental impact and mechanical behavior study of experimental road made with river sediments: recycling of river sediments in road construction, *J. Mater. Cycles Waste Manag.* 19 (2017) 1405–1414, <https://doi.org/10.1007/s10163-016-0529-5>.
- [57] A. Djalmy, M. Rguig, M. Meliani, Optimization of the granular mixture of natural rammed earth using compressible packing model, *Sustain* 15 (2023), <https://doi.org/10.3390/su15032698>.
- [58] R. Zentar, D. Wang, N.E. Abriak, M. Benzerzour, W. Chen, Utilization of siliceous-aluminous fly ash and cement for solidification of marine sediments, *Constr. Build. Mater.* 35 (2012) 856–863, <https://doi.org/10.1016/j.conbuildmat.2012.04.024>.
- [59] J.-M. Fleureau, J.-C. Verbrugge, P. Huergo, AI aspects of the behaviour of compacted clayey soils on drying and wetting paths, *Can. Geotech. J.* 39 (2002) 1341–1357.
- [60] Y. Abriak, W. Maherzi, M. Benzerzour, Senouci, A. Valorization of Dredged Sediments and Recycled Concrete Aggregates in Road Subgrade Construction, 2023.
- [61] MOGHRAÏBI, I. Modélisation Du Comportement Mécanique Des Sédiments Traités et Étude d'une Nouvelle Voie de Leur Valorisation Par Des Géopolymères, 2018.
- [62] M.E.G. Dobrovolski, G.S. Munhoz, E. Pereira, R.A. Medeiros-Junior, Effect of crystalline admixture and polypropylene microfiber on the internal sulfate attack in portland cement composites due to pyrite oxidation, *Constr. Build. Mater.* 308 (2021), 125018, <https://doi.org/10.1016/j.conbuildmat.2021.125018>.
- [63] Davy, J. *Etude Des Risques d' Oxydation de La Pyrite Dans Le Milieu Basique Du Béton*, 1996, 97–107.
- [64] T. Chompoorat, S. Likitlersuang, T. Thepumong, W. Tanapalungkorn, P. Jamsawang, P. Jongpradist, Solidification of sediments deposited in reservoirs with cement and fly ash for road construction, *Int. J. Geosynth. Gr. Eng.* 7 (2021) 1–12, <https://doi.org/10.1007/s40891-021-00328-0>.
- [65] T. Chompoorat, T. Thepumong, A. Khamplo, S. Likitlersuang, Improving mechanical properties and shrinkage cracking characteristics of soft clay in deep soil mixing, *Constr. Build. Mater.* 316 (2022), 125858, <https://doi.org/10.1016/j.conbuildmat.2021.125858>.
- [66] M.U. Hossain, C.S. Poon, I.M.C. Lo, J.C.P. Cheng, Comparative environmental evaluation of aggregate production from recycled waste materials and virgin sources by LCA, *Resour. Conserv. Recycl.* 109 (2016) 67–77, <https://doi.org/10.1016/j.resconrec.2016.02.009>.
- [67] E. Batuecas, I. Ramón-Álvarez, S. Sánchez-Delgado, M. Torres-Carrasco, Carbon footprint and water use of alkali-activated and hybrid cement mortars, *J. Clean. Prod.* 319 (2021), <https://doi.org/10.1016/j.jclepro.2021.128653>.
- [68] H. Zhang, C. Zhang, B. He, S. Yi, L. Tang, Recycling fine powder collected from construction and demolition wastes as partial alternatives to cement: a comprehensive analysis on effects, mechanism, cost and CO<sub>2</sub> emission, *J. Build. Eng.* 71 (2023), 106507, <https://doi.org/10.1016/j.jobbe.2023.106507>.
- [69] A. Singh, P. Vaddy, K.P. Biligiri, Quantification of embodied energy and carbon footprint of pervious concrete pavements through a methodical lifecycle assessment framework, *Resour. Conserv. Recycl.* 161 (2020), 104953, <https://doi.org/10.1016/j.resconrec.2020.104953>.
- [70] E. El-Seidy, M. Chougan, M. Sambucci, M.J. Al-Kheetan, I. Biblioteca, M. Valente, S. Hamidreza Ghaffar, Lightweight alkali-activated materials and ordinary portland cement composites using recycled polyvinyl chloride and waste glass aggregates to fully replace natural sand, *Constr. Build. Mater.* 368 (2023), 130399, <https://doi.org/10.1016/j.conbuildmat.2023.130399>.
- [71] Q. Tushar, S. Salehi, J. Santos, G. Zhang, M.A. Bhuiyan, M. Arashpour, F. Giustozzi, Application of recycled crushed glass in road pavements and pipeline bedding: an integrated environmental evaluation using LCA, *Sci. Total Environ.* 881 (2023), 163488, <https://doi.org/10.1016/j.scitotenv.2023.163488>.
- [72] UNPG-Union nationale des producteurs de granulats Module d'information Environnementale de La Production de Granulats à Partir de Roches Massives, 2017.
- [73] ADEME *Réalisation de Bilans Des Émissions de Gaz à Effet de Serre Utilisation Des Modules d'informations Environnementales*, 2012.
- [74] IFEU; SGKV *Analyse Comparative de La Consommation d'énergie et Des Émissions de CO<sub>2</sub> Entre Le Transport Routier et Le Transport Combiné Rail/Route*, 2002, 16.